Published in "Macromolecules 41(21): 8130–8137, 2009"
which should be cited to refer to this work.

Structure−Properties Relationship in Proton Conductive Sulfonated Polystyrene−Polymethyl Methacrylate Block Copolymers (sPS−PMMA)

Laurent Rubatat,[†,‡] Chaoxu Li,[†] Hervé Dietsch,[†,§] Antti Nykänen,[||] Janne Ruokolainen,[||] and Raffaele Mezzenga*[,†,⊥]

Department of Physics and Fribourg Center for Nanomaterials, University of Fribourg, Ch. du. Musée 3, CH-1700 Fribourg, Switzerland, Adolphe Merkle Institute, University of Fribourg, Ch. du. Musée 3, CH-1700 Fribourg, Switzerland, Department of Engineering Physics, Helsinki University of Technology, P.O. Box 5100, 02015 TKK, Finland, and Néstlé Research Center, Vers-Chez-Les-Blanc, 1000 Lausanne 26, Switzerland

ABSTRACT: We report on the dependence of proton conductivity on the morphologies of sulfonated polystyrene−poly(methyl methacrylate) (sPS−PMMA) diblock copolymers. Three different diblock copolymers of varying molecular weight and block volume fraction were studied, and for each one several sulfonation degrees of the PS block were considered. The investigation of the morphologies of the self-assembled sPS−PMMA diblocks was carried out in both dry samples and samples saturated with water, by means of small angle neutron scattering (SANS), transmission electron microscopy (TEM) and cryoTEM. Depending on molecular weight and sulfonation degrees, isotropic phase (ISO), lamellar phases (LAM), cylindrical hexagonal phase (HEX) and hexagonally perforated lamellae (HPL) were observed. The lamellar morphologies underwent marked volume expansion upon water pick up, while negligible swelling was detected for the other morphologies. Proton conductivity was measured in both the dry and wet states, the latter conditions resulting in an enhancement of conductivity up to 3 orders of magnitude. In particular it was shown that the conductivity, normalized by the volume fraction of the conductive domains (formed by PS, sPS and water), rises monotonically with the content of sulfonic groups, and with the following sequence of morphologies: ISO → HEX → HPL → LAM, accompanied by discontinuities in correspondence of order-to-order and order−disorder transitions.

1. Introduction

Ion exchange films are of prime interest as solid electrolytes for applications such as fuel cell, water treatment and related proton transport applications. Mechanical and chemical stability, combined to high ionic selectivity and transport efficiency are fundamental requirements for such applications. Because hydrophobic domains are usually responsible for mechanical stability while the hydrophilic domains provide transport capabilities, a compromise has generally to be found in the design of efficient proton conductive membranes.

During the last three decades, a considerable amount of studies has been dedicated to the understanding of the correlation between the morphology and the transport properties in ionomer materials and most often with specific regard to Nafion™ which remains up today the reference material for membranes used in fuel cell applications.[1−4] Despite all the studies devoted to the subject, however, the morphology of Nafion remains a point of high debate due to the difficulty of probing the structure at the length scale of few nanometers on this poorly ordered material.[1,5] More recently the use of block copolymers has been proposed as model systems for a better control of the morphology and consequently, to gain a better understanding on the proton transport mechanisms.[6−9]

A vast range of proton conductive block copolymer systems have been studied, including partially or fully sulfonated polystyrene: partially sulfonated poly(styrene-*b*-[ethylene-*co*-butylene]-*b*-styrene) copolymer (S−SEBS),[10−19] sulfonated poly(styrene-*b*-isobutylene-*b*-styrene) block copolymer (S−SIBS),[6,7] sulfonated hydrogenated poly(butadiene-*b*-styrene) diblock copolymer (S-HPBS),[20,21] sulfonated poly(styrene-*b*-[ethylene-*co*-propylene]) (S−SEP),[22−24] sulfonated poly(styrene-*b*-ethylene/propylene-*b*-styrene) (S−SEPS),[22] sulfonated poly-([vinylidene difluoride-*co*-hexafluoropropylene]-*b*-styrene) block copolymers (P[VDF-*co*-HFP]-*b*-SPS),[9,25,26] sulfonated poly-(styrene-*b*-methylbutylene) (SPS-*b*-PMB).[8]

It is well-known that in regular block copolymers, varying the volume fraction of the blocks and the segregation parameter, leads to controlled morphologies such as lamellae, hexagonal packed cylinders, bicontinuous double gyroid, close packed spheres, etc.[27,28] The structural studies performed on ionomer block copolymers, however, have revealed systematic inconsistencies with the regular theory on the block copolymers (phase diagram). Although the main sources of differences between standard and ionomer block copolymers may be found on the polyelectrolytic nature of the proton conductive block, the physics of self-assembly and the structure−properties relationship in this class of block copolymers has not yet been completely rationalized.

The aim of the present study is to bring new insight on the effect of the controlled addition of proton donating ionic moieties in the self-assembly of block copolymers. We have restricted our investigation to polystyrene-*block*-poly (methyl methacrylate) block copolymers, and have investigated the influence of the volume fraction between the two blocks as well

* To whom correspondence should be addressed at the Department of Physics and Fribourg Center for Nanomaterials, University of Fribourg (e-mail raffaele.mezzenga@unifr.ch; telephone + 41 26 300 9066; fax + 41 26 300 9747) or Nestlé Research Center (e-mail raffaele.mezzenga@rdls.nestle.com; telephone + 41 21 785 8078; fax + 41 21 785 8554.
[†] Department of Physics and Fribourg Center for Nanomaterials, University of Fribourg.
[‡] Present address: EPCP, UMR IPREM 5254, Université de Pau, Technopole Hélioparc 2 av. du président Angot, 64053 Pau Cedex 9, France.
[§] Adolphe Merkle Institute, University of Fribourg.
[||] Department of Engineering Physics, Helsinki University of Technology.
[⊥] Néstlé Research Center.

Table 1. Characteristics of PS-*b*-PMMA Used in This Study

series	M_n (g/mol)	M_w/M_n	ϕ_{PS} (vol %)[a]
S1	20,000	1.05	52.7
S2	52,500	1.09	21.8
S3	78,000	1.06	15.5

[a] Assuming additivity of volumes and the densities of PS and PMMA at room temperature ρ_{PS} of 1.05 g/cm^3 and ρ_{PMMA} of 1.17 g/cm^3, respectively.[36]

as the degree of sulfonation of the polystyrene block. The relationship between proton conductivity and the structure of the block copolymers in bulk is given and discussed.

2. Experimental Section

2.1. Materials. Three diblock copolymers of polystyrene-*block*-poly(methyl methacrylate) labeled as S1, S2 and S3 were purchased from Polymer Source Inc. (see Table 1 for their number-average molecular weights (M_n), polydispersities (M_w/M_n) and volume fractions of the PS block (ϕ_{PS})). Analytical sulfuric acid (98%), acetic anhydride and 1,2-dichloroethane were purchased by VWR (Germany) and used without further purification.

2.2. Sulfonation Procedure. Sulfonation of the PS block of the diblock copolymers was carried readapting a protocol reported in previous literature[25,26] and consists of the following steps: first PMMA-PS solutions are prepared dissolving the desired diblock copolymer into a common solvent for both blocks: 1,2-dichloroethane. In a typical synthesis, 0.5 g of the desired block copolymer is dissolved into 30 mL of 1,2-dichloroethane under vigorous stirring, and the so-obtained solution is maintained at 40 °C under reflux of an inert gas (Ar). Then, 2 mL of acetic anhydride are diluted into 5 mL of 1,2-dichloroethane at 0 °C under Argon flow into a parallel round-bottom flask. Then 1 mL of sulfuric acid is added slowly to this solution, resulting in the desired sulfonation agent solution: acetyl sulfate in 1,2-dichloroethane.[29] The 1,2-dichloroethane is used to decrease the viscosity of this solution, and it is preferable to prepare this acetyl sulfate solution with a small excess of acetic anhydride to inhibit the activity of any residual water possibly present in the reaction. The acetyl sulfate solution thus obtained is added dropwise to the block copolymer solution. Aliquots of the obtained solution are quenched into water and dried at different time t controlling the degree of sulfonation of the polystyrene block. The sulfonation times t used for all the series were 1.5, 5, and 10 h. The corresponding sulfonation degrees were successively precisely quantified by means of ^{1}H NMR analysis (see Table 2).[25,26] The samples were divided into three series (S1, S2, and S3), based on the original PS-*b*-PMMA block copolymers used for the sulfonation. Within each series, the numbers x (i.e., S1_*x*) is used to identify the sulfonation degree, and thus, rank their sulfonic groups content. For S1_34, the minimum content of sulfonic group (34%) is estimated by linear extrapolation from S1_10 and S1_20 data.

2.3. Water Uptake Measurement Protocol. Water uptake by weight was measured with an analytic balance (Mettler Toledo, model AG 204). The vapor-annealed samples (15−20 mg) were first equilibrated within saturated water vapor for 6 days. The samples were then removed and immediately weighted yielding the wet weight (W_w). Then after drying at 60 °C for 24 h under ultra high vacuum (10^{-8} mbar), the samples were weighted yielding the dry weight (W_d). The weight uptake was calculated by the following equation: water uptake (%) = 100 ($W_w - W_d$)/W_d.

2.4. Annealing Procedures. Samples were annealed following two different procedures, thermally or through solvent vapor. Thermally annealed samples were prepared by annealing the block copolymer samples at 160 °C for 48 h under ultra high vacuum (10^{-8} mbar). Vapor-annealed samples were prepared by casting 1 wt % THF solutions onto quartz substrates as films (with a thickness of ca. 100−300 μm). Then the films were kept in saturated THF vapor at room temperature for 48 h and subsequently thermally annealed at 70 °C (e.g., lower than glass transition of PS and PMMA) for ca. 24 h under ultrahigh vacuum.

2.5. Transmission Electron Microscopy (TEM) and Cryo-TEM. After being glued on microtome sample holder tips, samples were cryo-sectioned by a diamond knife with a Leica Ultracut UCT ultramicrotome at ca. −20 °C. The sections with a thickness of 50 nm were collected onto 400 mesh copper grids and then stained by RuO_4 for 20 min. The sections prepared as such were ready for TEM study on dry samples. Transmission electron microscopy (TEM) images were obtained with a Philips TEM (CM 100) instrument operating at a voltage of 80kV. For cryo-TEM study on wet samples, unstained sections were exposed to saturated water vapor environment at room temperature for 48 h, then aqueous 0.5% solution of ruthenium tetraoxide was added and sections were stained for 30 min. This protocol allows staining the sPS and PS domains after water pick up has reached a saturation in the samples, e.g. without interfering with the swelling of the samples. After staining, sections were transferred to a water-vapor saturated environmental chamber FEI vitrobot, and vitrified in a mixture of liquid ethane/propane (−180 °C). Vitrified samples were cryo-transferred into FEI Tecnai 12 transmission electron microscope using Gatan 910 cryo-transfer holder, whose temperature was maintained at −185 °C. Samples were imaged by TEM operated at an acceleration voltage of 120 kV using bright field mode. Micrographs were recorded using Gatan UltraScan 1000 camera having CCD size of 2048 × 2048 pixels.

2.6. Small Angle Neutron Scattering (SANS). Small-angle neutron scattering (SANS) measurements were performed at the Swiss spallation neutron source SINQ (PSI, Villigen) on the SANS II beam line. Vapor-annealed samples were laid into 1 mm-thick Hellma quartz cell. Both dry films and films swollen in deuterated water (for at least 12 h before measurement) were investigated by SANS. The data were collected by a two-dimensional detector located at three different sample-to-detector distances: 1.2, 2, and 6 m, respectively, with corresponding neutron wavelengths of 4.55, 4.55, and 6.37 Å and collimation tubes of 2, 2, and 6 m. Raw data were corrected for empty cell, solvent-filled cell, sample-filled cell and electronic noise background by using standard procedures. Data were then azimuthally averaged to get the scattering intensity, I, in arbitrary unit, versus the scattering vector q (nm^{-1}) defined as $q=4\pi/\lambda[\sin(\theta/2)]$, with θ the scattering angle.

2.7. Proton Conductivity Measurements. AC proton conductivity was measured via electric bridge measurement with an oscilloscope (HP 54540C). Samples were casted as films (with the thickness of 100∼500 μm) from 1 wt % THF solutions onto glass substrates, which were partially sputtered by gold with a mask to yield four electrodes for four-probe conductivity measurements. After casting, the films underwent the exact same annealing conditions used for TEM and SANS samples, that is: (a) dry films were kept in saturated THF vapor at room temperature for 48 h and thermally annealed at 70 °C for ca. 24 h in vacuum; (b) the wet samples were prepared by further exposing the films with saturated water vapor at room temperature for 48 h. An alternating voltage of ∼1 V was applied at a constant frequency of 50 Hz. Equation $G=\sigma A/l$ is used to obtain the conductivity (σ), where G is the conductance, A is the cross-sectional area, and l is the gold electrode fixed distance.

3. Results and Discussion

For PS-*b*-PMMA diblock copolymers, the Flory−Huggins interaction parameter χ, was measured by Russell et al.[30] to be $\chi = 0.028 \pm 0.002 + (3.9 \pm 0.06)/T$, where T is the absolute temperature. At 120 °C, which is the lowest thermal annealing temperature used in the present study, due to the glass transitions of PS and PMMA, the product χN for the block copolymer S1 is 7.4. According to mean-field phase diagram[27] the block copolymer should lie in the disordered state. This was also confirmed by separate small-angle X-ray scattering measurements and the TEM images (not shown in the present paper). However, after sulfonation, it shows ordered lamellar structures, provided that the sulfonation degree is high enough. Figure 1 shows the TEM image of the thermally annealed S1_34, whose

Table 2. Morphologies and Wet Conductivity of Block Copolymers Used in This Study

				morphologies		
					vapor annealing	
samples	IEC (mmol/g)	water uptake (%)	conductivity (S/cm)	thermal annealing	dry	swollen
S1_0	0	–	9.1×10^{-7}	disorder	disorder	disorder
S1_10	0.547	7.4	1.6×10^{-4}	disorder	disorder	disorder
S1_20	1.66	48	4.0×10^{-3}	disorder	lamellar	lamellar
S1_34	–	–	–	lamellar	lamellar	–
S2_0	0	–	8.5×10^{-7}	disorder	disorder	disorder
S2_11	0.174	4.8	2.2×10^{-5}	disorder	disorder	disorder
S2_17	0.353	11.7	1.3×10^{-4}	disorder	hexagonal	hexagonal
S2_35	0.766	18	3.6×10^{-4}	disorder	HPL	HPL
S3_0	0	–	9.9×10^{-7}	disorder	disorder	disorder
S3_9	0.147	3	1.8×10^{-6}	disorder	disorder	disorder
S3_15	0.264	10.6	4.0×10^{-5}	disorder	disorder	disorder
S3_37	0.564	17.5	1.8×10^{-4}	disorder	HPL	HPL

sulfonation degree has reached a minimum of 34%. Although onset of degradation is observed (change in color from transparent to brownish), a lamellar phase is shown where the sPS-*co*-PS blocks selectively stained by RuO_4 appear dark, while the PMMA blocks appear white. A similar sulfonation-induced ordering effect on the microsctructure was also observed by Mani et al. in other block copolymer systems.[31] The most plausible reason that can be advanced for this sulfonation-induced ordering is an increased Flory−Huggins interaction parameter χ with consequent increase in the degree of segregation χN in sPS-*co*-PS-*b*-PMMA, with respect to PS−PMMA.

In order to promote microphase separation without possible degradation occurring from the presence of sulfonic groups at high temperatures, the samples were kept in saturated THF vapor at room temperature for 48 h. Then the samples were dried at 70 °C (well below the T_g of each block) for ca. 24 h in vacuum to remove all residual solvent. THF was expected to promote the molecular mobility at low temperature. Furthermore, the segregation parameter is expected be to larger at lower temperatures, which should also favor microphase separation as compared to thermal annealing at temperatures above the T_g of all components. The TEM images for the ordered samples observed after vapor annealing are shown in Figure 2. As shown in Figure 2a, the sulfonated S1_20 (IEC =1.66 mmol/g) showed a lamellar structure. In particular, this sample lays within the disordered state after annealing at 160 °C whereas it shows lamellar ordering after vapor annealing. Similarly, although all the sulfonated S2 and S3 samples were in the isotropic disordered state after thermal annealing, the vapor-annealing samples microphase separated when the sulfonation degree reached values of 17% and 35% for series 2 and 37% for series 3 (check Table 2 for the corresponding IEC). A careful analysis of Figures 2b-d, reveals hexagonal-packed cylinders for samples S2_17, and hexagonally perforated lamellae (HPL) for S2_35 and S3_37. The attribution of the morphologies to HPL phases is based on the inversion of the contrast (black cylinders → white cylinders) occurring in the images and the presence of two main periodicities in the images (attributed to the period between lamellae and the period between perforating cylinders, respectively).

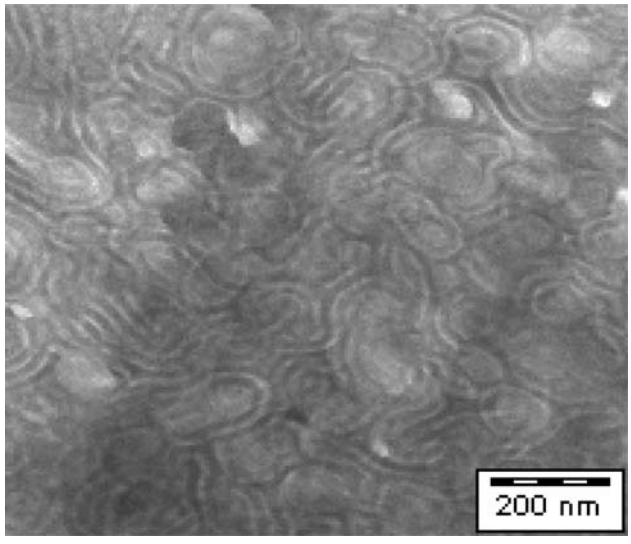

Figure 1. TEM image of S1_34 after annealing at 160 °C for 48 h.

Although HPL in diblock copolymers has been reported on thin films with preferential wetting surfaces,[32] the existence of HPL in pure diblock copolymers in bulk is not thermodynamically possible, as it corresponds to metastable local minima of the total free energy. Nevertheless, HPL phases in bulk diblock copolymers have been observed despite very long annealing times in block copolymers of the type polypropylene-*block*-poly(ethylene-*co*-propylene)[33] or polystyrene-*block*-poly(ethylene-*co*-propylene)[31] in which one of the two blocks consists of a statistic block with A and B species, exactly as in the present case (e.g., styrene and sulfonated styrene). Other examples of HPL phases have been reported in supramolecular complexes of phenolated alkyl tails with PS-*b*-P_4VP block copolymers[34] in which, high annealing temperatures may partially break the hydrogen bonding between the phenol and P_4VP groups leading to nonstoichimetric complexation. The resulting partially complexed PV2P block can also be assimilated to a random copolymer of A and B species, which again bears similarities with the system presently investigated here, as one block is a random copolymer, giving an architecture of the type A-*co*-B-*block*-C.

Parts a, b, and c of Figures 3 present the SANS spectra measured on vapor-annealed samples for series S1, S2, and S3, respectively. The intensities are relatively weak due to a poor contrast between the PMMA and the PS domains, with respective scattering length density of 1.05×10^{10} and 1.41×10^{10} cm·cm^{-3}. We are focusing on the peak visible between 0.2 and 0.4 nm^{-1}. For all three series, the neat PS−PMMA prior to sulfonation shows no peak, in agreement with isotropic disordered homogeneous phases. Apart from sample, S1_10, however, a peak appears in all the series, as soon as sulfonation is carried out on the block copolymers. This would suggest that for the S2 and S3 series, microphase separation is initiated already at an earlier sulfonation stage than what is detectable using solely TEM microscopy. The SANS peak is shifting toward small angles as the sulfonation degree is increasing, as could be expected due to the increase in the volume of the sulfonate groups. Nonetheless, in previous works Gromadski et al. [24] and Lu et al. [14] showed that increasing the sulfonation degree leads to a slight decrease of the *d*-spacing,

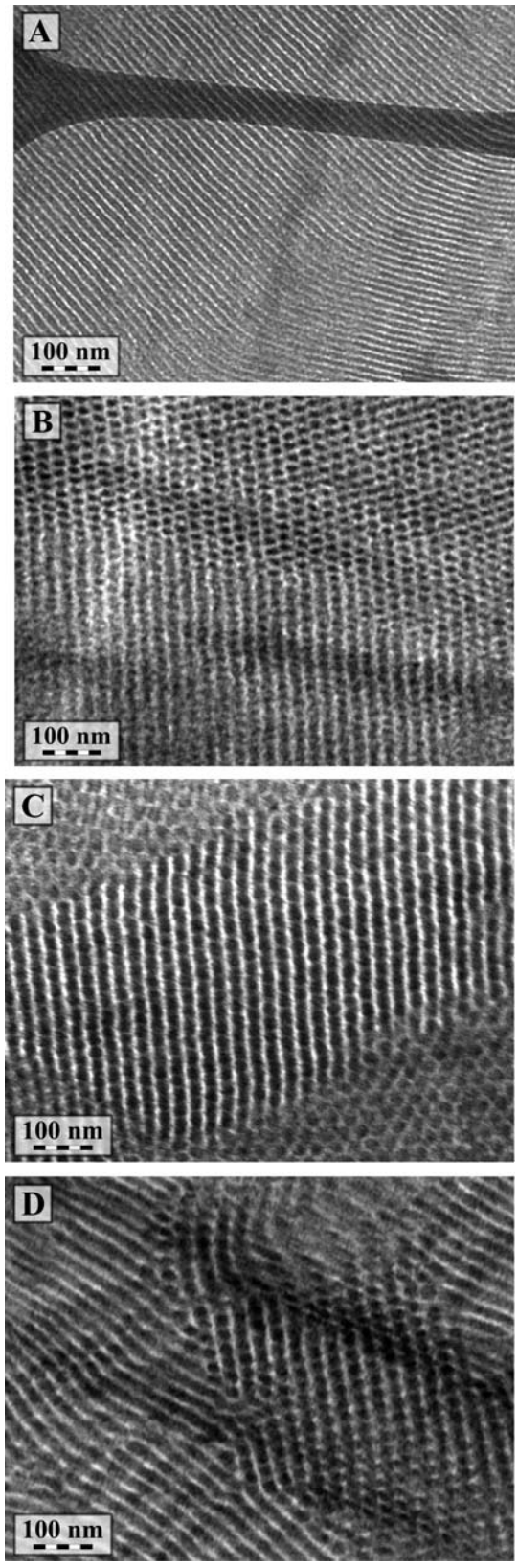

Figure 2. TEM images of vapor annealing for samples: (a) S1_20, (b) S2_17, (c) S2_35 and (d) S3_37.

which suggests that peak positioning with sulfonation degree may-be system sensitive and that no general conclusions can be drawn on its evolution. All the correlation distances calculated from the q-position of the peaks using the Bragg relation, $D = 2\pi/q$, are presented in Table 3.

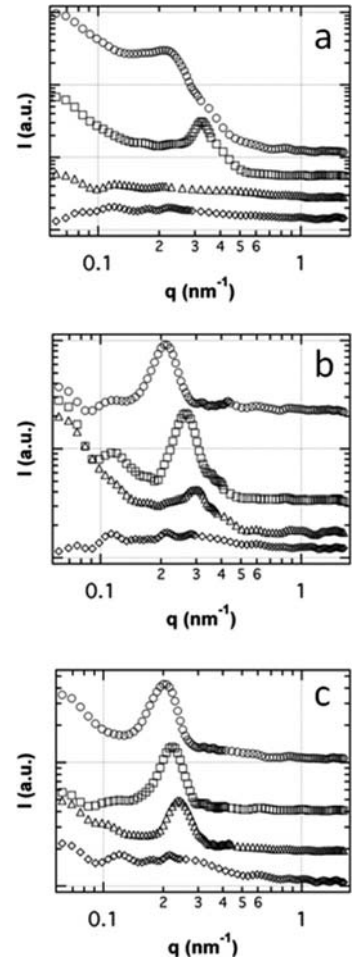

Figure 3. SANS spectra measured on films series S1 (a), S2 (b), and S3 (c) at ambient conditions. The PS block sulfonation degrees are corresponding to the following group sulfonation percentage 0 (diamond), ≈10 (triangle), ≈20 (square) and ≈35 (circle). For the exact sulfonation percentages refer to Table 2.

Table 3. Correlation Distances in nm Calculated from the SANS Peak Positions Using the Bragg Relation As a Function of the Approximate Degree of Sulfonation (D.S.)

series	samples	*d*-spacing (nm) dry	*d*-spacing (nm) swollen
S1	S1_0		
	S1_10		16.7
	S1_20	19.4	25.7
	S1_34	28.3	
S2	S2_0		
	S2_11	20.8	21.3
	S2_17	23.6	23.6
	S2_35	30.3	31.4
S3	S3_0		
	S3_9	25.7	-
	S3_15	28.3	28.2
	S3_37	30.3	31.4

Parts a, b, and c of Figures 4 present the SANS spectra measured on membranes swollen in D_2O at ambient condition for series S1, S2, and S3, respectively. The intensities are greatly enhanced owing to the absorption of D_2O from the sPS domains of the block copolymers. In most cases a correlation peak is observable on the scattering curves in the region ranging from 0.2 to 0.4 nm^{-1}. Consistently with the dried homologue series, the peak is also shifting toward smaller angles as the sulfonation degree is increasing, owing to the increased tendency to water pick up and swelling with sulfonation degree. It is to be noted that no peak is present on the scattering curve measured on the S1_34 sample, as a consequence of excessive swelling for this

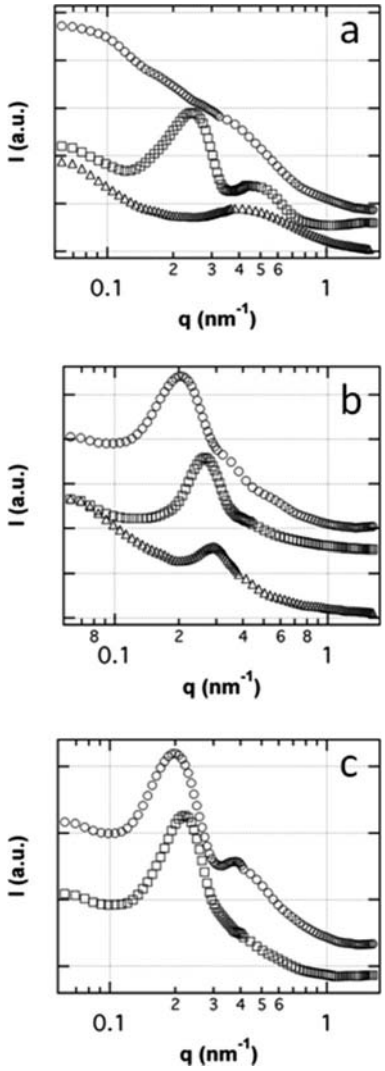

Figure 4. SANS spectra measured on films series S1 (a), S2 (b), and S3 (c) swollen in D_2O. The PS block sulfonation degrees are corresponding to the following group sulfonation percentage ≈10 (triangle), ≈20 (square), and ≈ 35 (circle). For the exact sulfonation percentages refer to Table 2.

sample, whose behavior in water resembles that of hydrogels. A second order peaks is observable on the S1_20 and S3_37 samples. In the case of S1_20, the second reflection occurs at $2q^*$, which is consistent with a lamellar phase, as expected based on TEM study. For the S3_37 sample, however, the second reflection occurs at a value intermediate between that expected for hexagonally packed cylinder morphology, e.g., $\sqrt{3}q^*$ and a lamellar morphology, e.g., $2q^*$. More precisely, the peaks/shoulders occurs at $1.87q^*$, which indicates that the two reflections are not directly correlated, as can happen in HPL morphologies (where one peak can possibly indicate the period between lamellae and the other the period in between perforating cylinders).

Figure 5 compares the scattering curves measured in both dry conditions and swollen in D_2O for S1_20 (a), S2_17 (b), and S3_37 (c) series. While a minimum-to-nil shift toward smaller angles occurs on samples from series S2 and S3 after swelling, sample from the series S1 presents a notable shift indicating a significant increase (37%) of the correlation distance after swelling, as well as the appearance of a second order peak at $2q^*$ (lamellar morphology). If the water pick up is known by separate experiments, the ratio in the lamellar spacing before and after hydration can be easily evaluated. Indeed, the lamellar morphology is formed by two domains: (i) the PS, sPS and

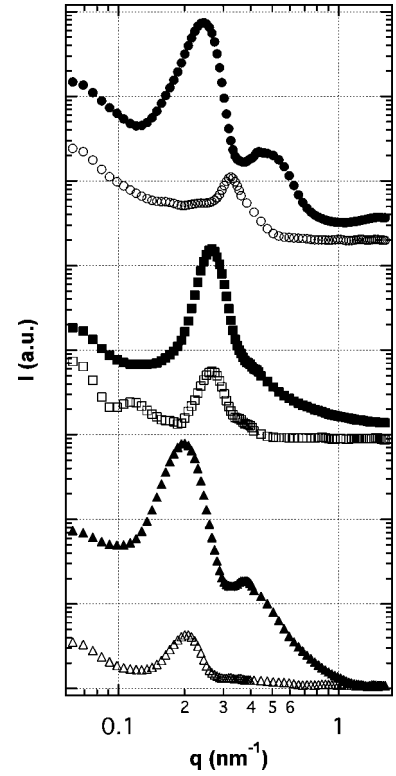

Figure 5. SANS spectra measured on films from the S1_20, S2_17, and S3_37 samples. The films are equilibrated at dry conditions (open marker) and swollen in D_2O (solid marker). Samples S1_20, S2_17, and S3_37 are respectively represented by circle, square, and triangle.

adsorbed water and (ii) the PMMA. The swelling ratio among the volumes of the hydrated and dry lamellar phases is simply equal to ratio between the periods of the lamellar spacing after ($D_{hydrated}$) and before (D_{dry}) water uptake. Thus, from the densities and molecular weight of the individual constituents one can write:

$$\frac{D_{hydrated}}{D_{dry}} = \frac{\dfrac{M_{PS}}{\rho_{PS}} + \dfrac{M_{sPS}}{\rho_{sPS}} + \dfrac{M_{H2O}}{\rho_{H2O}} + \dfrac{M_{PMMA}}{\rho_{PMMA}}}{\dfrac{M_{PS}}{\rho_{PS}} + \dfrac{M_{sPS}}{\rho_{sPS}} + \dfrac{M_{PMMA}}{\rho_{PMMA}}} = \frac{\dfrac{M_{PS}}{\rho_{PS}} + \dfrac{M_{sPS}}{\rho_{sPS}} + P_{w.u.}\dfrac{M_{PS}+M_{sPS}+M_{PMMA}}{\rho_{H_2O}} + \dfrac{M_{PMMA}}{\rho_{PMMA}}}{\dfrac{M_{PS}}{\rho_{PS}} + \dfrac{M_{sPS}}{\rho_{sPS}} + \dfrac{M_{PMMA}}{\rho_{PMMA}}} \quad (1)$$

where the M_x and the ρ_x are the molar mass and the density of the constituents, respectively. Here M_{H2O} corresponds to the mass of water partitioning within one mole of copolymer. Using these basic calculations, the data measured on sample S1_20 can be analyzed, since this series shows lamellar morphology both before and after hydration. Using 0.48 for the water uptake, $P_{w.u.}$, (see Table 2) and using 1.00 g/cm,^{3} 1.05 g/cm^3 1.05 g/cm^3 and 1.17 g/cm^3 the densities for H_2O, PS, sPS and PMMA, respectively and 8000, 3540 and 10000 for M_{PS}, M_{sPS} and M_{PMMA}, respectively, a ratio of 1.53 is found. On the basis of SANS data, the lamellar period is evaluated at 19 and 26 nm for the dry and swollen film, respectively, which gives $D_{hydrated}/D_{dry} = 1.37$. Thus the swelling measured by SANS is slightly lower than that measured by water pick-up experiments. This is to be expected considering the different experimental protocols used to swell films in the two experi-

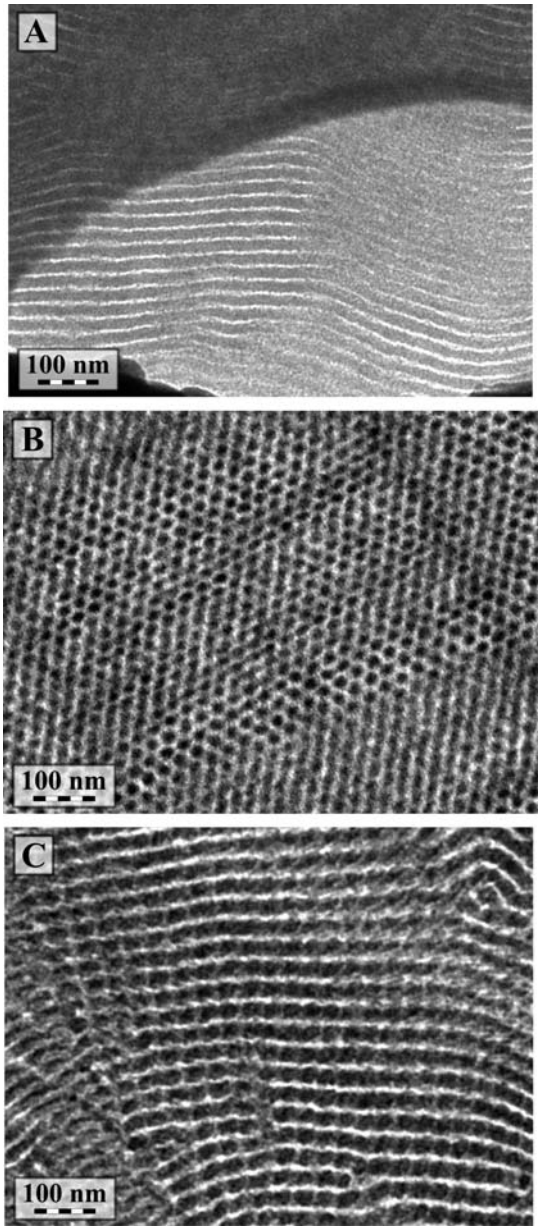

Figure 6. Cryo-TEM images for (a) S1_20, (b) S2_17, and (c) S3_37 samples.

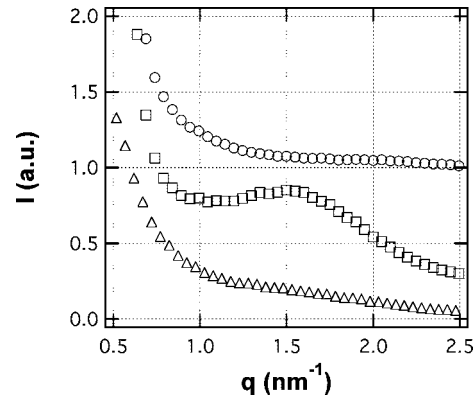

Figure 7. Wide angle neutron scattering spectra measured on film series S1 swollen in D_2O. The PS block sulfonation degrees are corresponding to the following group sulfonation percentage ≈10 (triangle), ≈20 (square), and ≈ 35 (circle). For the exact sulfonation percentages refer to Table 2.

ments, e.g immerging films for SANS studies and vapor swelling for weight pick up measurements. Indeed, in order to precisely evaluate the relative water pick up on our small sized samples, vapor swelling was preferred to immersion, as this latter protocol would likely lead to an overestimation of the wet mass (water present on the surface after wiping with paper filters). Furthermore, while H_2O is used for the vapor swelling experiments, D_2O is used for the SANS experiments. Slightly different binding mechanisms of D_2O to sPS domains compared to H_2O, can also be envisaged, and therefore, in view of these considerations, the swelling of sulfonated block copolymers measured by SANS and weight pick-up have to be considered in reasonably good agreement.

In order to compare the SANS information in Figure 5a−c, with real space images, we performed cryoTEM on sulfonated S1, S2, and S3 series. Figure 6a−c shows the morphologies for S1_20, S2_17, and S3_37 series. Compared to Figure 2 no major changes occur with respect to S2 and S3 series consistently with data shown in Figure 5. However for S1, an increase in period of 50% resulting from water uptake can be noted (by direct measurement of periods in Figures 6a and 2a), which is in good agreement with the increase in period estimated by combining water uptake measurements and eq. 1 (53%). More in details, by comparing Figure 2a and Figure 6a, it can be observed that while the white PMMA domains remain of nearly unaffected width, the width of the black sPS-*co*-PS increase, as a result of water partitioning within these domains only.

Scattering at larger angles was also probed by neutron scattering, in the 0.5−2.5 nm^{-1} region. Usually, it is in this q-range that the well-known ionomer peak is expected. Figures 7 shows respectively the scattering curves measured on series S1. This peak is visible only on sample S1_20 at 1.5 nm^{-1}, which corresponds to about 5 nm in the direct space, in agreement with the ionomer literature.[35] The S1_34, does not present ionomer peak due to excessive swelling and partial dissolution in water. Samples from series S2 and S3 showed no ionomer peak, likely due to the poor water uptake in those series.

It is known that water absorption, which is correlated with the sulfonation degree, greatly changes the physical properties of ionomers, such as ionic conductivity. In the dry state at room temperature, the sulfonic groups are essentially not deprotonated and the resulting conductivity, is very low, on the order of 10^{-7} $S \cdot cm^{-1}$. After swelling in water, deprotonation of sulfonated groups is triggered, and mobility greatly enhanced, leading to rapid increase of ion conductivity with sulfonation content as shown in Table 2. However, the conductivity depends not only on the sulfonation degree of the block copolymers but also on their morphologies, as previously observed by Kim et al.[12] Whereas a clear difference can be expected for conductivity arising in disordered phases, cylindrical phases and lamellar phases, consistently with hopping, 1D and 2D transport mechanisms, respectively, the difference occurring between a lamellar phase and hexagonally perforated lamellae is less straightforward and to the best of our knowledge, has not been reported in literature yet.

To study the effect of block copolymer structure on proton transport, Figure 8 shows the normalized proton conductivity per volume fraction of the swollen sPS-*co*-PS domains, σ/Φ, as a function of the sulfonation degree, where Φ is the volume fraction of the PS + sPS + water domains. Not only, it can be seen that the normalized conductivity rises with the degree of sulfonation, but this also grows systematically when going from ISO to HEX to HPL to LAM phases. This becomes even more evident when comparing samples with nearly identical sulfonation degrees. For examples, samples with sulfonation degree ranging between 15 and 20%, show a systematic increase in

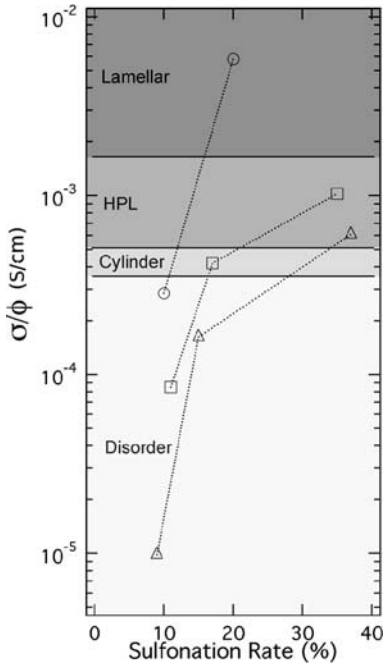

Figure 8. The normalized proton conductivity σ/Φ as a function of the sulfonation degree for the three series: S1 (circle), S2 (square), and S3 (triangle). Φ refers to the volume fraction of the PS + sPS + water domains.

the normalized conductivity when going from ISO → HEX → LAM phases, consistently, with hopping, 1D and 2D transport mechanisms.

Very illustrative is also the comparison between conductivities of the HPL and the Lam morphologies. Indeed, although HPL samples possess higher sulfonation degree than the lamellar phase (about 35% versus 20%), their normalized conductivity remains much lower than for the lamellar case. The reduced conductivity of HPL morphologies compared to LAM morphologies is to be attributed to the appearance of the PMMA perforating cylinders within the sPS-*co*-PS layers. Furthermore, while the HPL have a negligible swelling due to the constraints exerted by the perforating PMMA cylinders, the lamellar phase has a much larger swelling and greater water uptake, which contributes directly to the increased efficiency in deprotonating sPS moieties and the mobility of the protons. This is also correlated with the presence of the ionomer peak which is clearly noticeable only on the S1_20 lamellar sample, indicating that also the organization of ionic moieties is crucial to efficiently build up conductivity.[9]

In summary, the observed variations of normalized conductivity are consistent with the changes in the structures of block copolymers and offer an additional tool to distinguish between different morphologies and to detect order-to-order and order−disorder transitions.

4. Conclusions

We have investigated the effect of controlled sulfonation degree on the self-assembly morphologies and proton conductivity of sulfonated polystyrene−poly(methyl methacrylate) (sPS-*co*-PS-*block*-PMMA) diblock copolymers, in both dry and wet states. Depending on molecular weight and sulfonation degrees, isotropic phase (ISO), lamellar phases (LAM), cylindrical hexagonal phase (HEX) and hexagonally perforated lamellae (HPL) were observed, and their topological changes were investigated by combining small angle neutron scattering (SANS), transmission electron microscopy (TEM) and cryoTEM. Samples with LAM morphologies underwent extensive period increase upon water exposure, while little to nil swelling was observed for samples with HEX or HPL morphologies. As expected, the water pick up was accompanied by a remarkable increase in proton conductivity; nonetheless, the increase of conductivity was different for different morphologies. By comparing the conductivity normalized by the overall volume fraction of the domains formed by sPS + PS + water, it was possible to distinguish among different morphologies, the normalized conductivity rising monotonically when going through the following morphologies: ISO → HEX → HPL → LAM, in agreement with hopping, 1D and 2D charges transport mechanisms. Thus, the proton conductivity, normalized by the volume fraction of the conductive domains offers an additional rational to distinguish among different morphologies within this class of self-assembled block copolymers.

Acknowledgment. We acknowledge the financial support of the Swiss Foundation Gebert Ruf Stiftung. We thank SINQ at PSI for the neutron experiment beamtime and Dr. Urs Gasser for his help with the setup. The authors want to thank Zhiqing Shi (CNRC Vancouver) for discussions on the polystyrene sulfonation chemistry.

References and Notes

(1) Diat, O.; Gebel, G. *Nat. Mater.* **2008**, *7*, 13.
(2) Gierke, T. D.; Munn, G. E.; Wilson, F. C. *J. Polym. Sci., Part B* **1981**, *19*, 1687.
(3) Rubatat, L.; Rollet, A. L.; Gebel, G.; Diat, O. *Macromolecules* **2002**, *35*, 4050.
(4) Schmidt-Rohr, K.; Chen, Q. *Nat. Mater.* **2008**, *7*, 75.
(5) Kreuer, K. D. *J. Membr. Sci.* **2001**, *185*, 29.
(6) Elabd, Y. A.; Napadensky, E.; Sloan, J. M.; Crawford, D. M.; Walker, C. W. *J. Membr. Sci.* **2003**, *217*, 227.
(7) Elabd, Y. A.; Walker, C. W.; Beyer, F. L. *J. Membr. Sci.* **2004**, *231*, 181.
(8) Park, M. J.; Downing, K. H.; Jackson, A.; Gomez, E. D.; Minor, A. M.; Cookson, D.; Weber, A. Z.; Balsara, N. P. *Nano Letters* **2007**, *7*, 3547.
(9) Rubatat, L.; Shi, Z. Q.; Diat, O.; Holdcroft, S.; Frisken, B. J. *Macromolecules* **2006**, *39*, 720.
(10) Ehrenberg, S. G.; Serpico, J. M.; Wnek, G. E.; Rider, J. N. US Patent, **1995**.
(11) Kim, J.; Kim, B.; Jung, B. *J. Membr. Sci.* **2002**, *207*, 129.
(12) Kim, J.; Kim, B.; Jung, B.; Kang, Y. S.; Ha, H. Y.; Oh, I. H.; Ihn, K. J. *Macromol. Rapid Commun.* **2002**, *23*, 753.
(13) Lee, W. J.; Jung, H. R.; Lee, M. S.; Kim, J. H.; Yang, K. S. *Solid State Ionics* **2003**, *164*, 65.
(14) Lu, X.; Steckle, W. P.; Weiss, R. A. *Macromolecules* **1993**, *26*, 5876.
(15) Lu, X. Y.; Steckle, W. P.; Hsiao, B.; Weiss, R. A. *Macromolecules* **1995**, *28*, 2831.
(16) Mauritz, K. A.; Storey, R. F.; Mountz, D. A.; Reuschle, D. A. *Polymer* **2002**, *43*, 4315.
(17) Mauritz, K. A.; Storey, R. F.; Reuschle, D. A.; Tan, N. B. *Polymer* **2002**, *43*, 5949.
(18) Weiss, R. A.; Sen, A.; Pottick, L. A.; Willis, C. L. *Polymer* **1991**, *32*, 2785.
(19) Weiss, R. A.; Sen, A.; Willis, C. L.; Pottick, L. A. *Polymer* **1991**, *32*, 1867.
(20) Mokrini, A.; Acosta, J. L. *Polymer* **2001**, *42*, 9.
(21) Mokrini, A.; Rio, C. D.; Acosta, J. L. *Solid State Ionics* **2004**, *166*, 375.
(22) Mani, S.; Weiss, R. A.; Williams, C. E.; Hahn, S. F. *Macromolecules* **1999**, *32*, 3663.
(23) Zhang, G.; Liu, L.; Wang, H.; Jiang, M. *Eur. Polym. J.* **2000**, *36*, 61.
(24) Gromadzki, D.; Cernoch, P.; Janata, M.; Kudela, V.; Nallet, F.; Diat, O.; Stepanek, P. *Eur. Polym. J.* **2006**, *42*, 2486.
(25) Shi, Z.; Holdcroft, S. *Macromolecules* **2005**, *38*, 4193.
(26) Shi, Z. Q. *Synthesis and Characterization of Proton Conducting, Fluorine-Containing Block Copolymers. Ph.D. Thesis*. Simon Fraser University, Burnaby, Canada, 2004.
(27) Leibler, L. *Macromolecules* **1980**, *13*, 1602.
(28) Matsen, M. W.; Bates, F. S. *Macromolecules* **1996**, *29*, 1091.
(29) Makowski, H. S.; Lundberg, R. D.; Singhal, G. H. U.S. Patent No. 3,870,841; **1975**.
(30) Russell, T. P.; Hjelm, R. P.; Seeger, P. A. *Macromolecules* **1990**, *23*, 890.
(31) Mani, S.; Weiss, R. A.; Hahn, S. F.; Williams, C. E.; Cantino, M. E.; Khairallah, L. H. *Polymer* **1998**, *39*, 2023.

(32) Park, I.; Park, S.; Park, H. W.; Chang, T.; Yang, H. C.; Ryu, C. Y. *Macromolecules* **2006**, *39*, 315.
(33) Ruokolainen, J.; Mezzenga, R.; Fredrickson, G. H.; Kramer, E. J.; Hustad, P. D.; Coates, G. W. *Macromolecules* **2005**, *38*, 851.
(34) Valkama, S.; Ruotsalainen, T.; Nykanen, A.; Laiho, A.; Kosonen, H.; ten Brinke, G.; Ikkala, O.; Ruokolainen, J. *Macromolecules* **2006**, *39*, 9327.
(35) Gierke, T. D.; Hsu, W. Y. *J. Am. Chem. Soc.* **1982**, 283.
(36) Van Krevelen, D. W. *Properties of Polymers*, Third completely revised ed.; Elsevier: Amsterdam, Lausanne, New York, Oxford, Singapore, Shannon, and Tokyo, 1997. Brandrup, J.; Immergut, E. H. *Polymer handbook*; Wiley: New York, 1975.